

See discussions, stats, and author profiles for this publication at: <https://www.researchgate.net/publication/5938192>

# Closed Mechanoelectrochemical Cycles of Individual Single-Chain Macromolecular Motors by AFM

ARTICLE *in* ANGEWANDTE CHEMIE INTERNATIONAL EDITION · NOVEMBER 2007

Impact Factor: 11.26 · DOI: 10.1002/anie.200702387 · Source: PubMed

---

CITATIONS

41

---

READS

22

6 AUTHORS, INCLUDING:



[Marina I Giannotti](#)

University of Barcelona

30 PUBLICATIONS 359 CITATIONS

SEE PROFILE



[Holger Schönherr](#)

Universität Siegen

202 PUBLICATIONS 4,900 CITATIONS

SEE PROFILE



[Gyula Julius Vancso](#)

University of Twente

277 PUBLICATIONS 6,459 CITATIONS

SEE PROFILE

# Closed Mechanoelectrochemical Cycles of Individual Single-Chain Macromolecular Motors by AFM\*\*

Weiying Shi, Marina I. Giannotti, Xi Zhang, Mark A. Hempenius, Holger Schönherr, and G. Julius Vancso\*

Dedicated to Prof. Dr. Ir. David N. Reinhoudt on the occasion of his 65th birthday

Natural molecular motors, including the proton pump in membranes,<sup>[1]</sup> motor proteins,<sup>[2]</sup> and flagellar motors in bacteria,<sup>[3]</sup> have been studied in great detail. Pioneering work led to insight into the fundamental molecular-scale processes and to the exploitation of natural motors in fascinating biomimetic applications; yet the proposed energy-conversion mechanisms and molecular aspects remain in many cases controversial.<sup>[4,5]</sup> Research on the synthetic counterparts of these motors,<sup>[6]</sup> including molecular switches<sup>[7]</sup> and machines,<sup>[8]</sup> has also recently witnessed significant advances.<sup>[9]</sup>

In this context, single-molecule studies may provide access to a more fundamental understanding of relevant molecular-scale processes that are also pertinent for the understanding of the natural counterparts. An outstanding example of the realization of a closed-loop optomechanical cycle was reported by Gaub and co-workers.<sup>[10]</sup> Single polyazopeptide chains were reversibly shortened against an external force in single-molecule force spectroscopy (SMFS) experiments by photochemical switching between *trans*- and *cis*-azobenzene isomeric configurations. The maximum efficiency of the cycle at the molecular level was estimated to be about 10%.

In previous work, we investigated stimulus-responsive poly(ferrocenylsilane) (PFS) polymers<sup>[11]</sup> as a model system for the realization of (macro)molecular motors powered by an electrochemical redox process.<sup>[12–14]</sup> Different segment lengths and elasticities for the neutral and oxidized forms of single PFS chains, achieved by electrochemical or wet

chemical redox chemistry, were observed by SMFS.<sup>[13,14]</sup> Differences in the elasticity of PFS polymers were also reported by the group of Zhang.<sup>[15]</sup> Based on these results, the work output and the corresponding efficiency of a model electromechanical cycle were calculated.

Even though a closed cycle was originally not reported, we proposed a motor based on an individual PFS macromolecule.<sup>[13,14,16]</sup> Such electrochemically driven, macromolecule-based motors are potentially interesting for the realization of single-molecule devices, as they can in principle be addressed on the single-molecule level by using miniaturized electrodes and can be repeatedly run in cycles in a reversible manner. In this context, it is important to determine how the efficiency of single motors depends on various experimental and (macro)-molecular design parameters. Hence, the analysis of closed electromechanical cycles of individual macromolecules is required, including the localization and addressing of a single macromolecule by an AFM tip, and the stretching and relaxing of the molecule in situ under different applied electrochemical potentials (Figure 1).

Herein, we report the first experimental realization of closed mechanoelectrochemical cycles of individual PFS chains in electrochemical AFM-based SMFS, and the quantitative analysis of the efficiency of the closed cycles as a function of extension. This work contributes to unraveling the relation of attainable single-molecule forces and efficiencies on the one hand and molecular structure and external parameters on the other, and hence forms the basis for the

[\*] W. Shi, Dr. M. I. Giannotti, Dr. M. A. Hempenius, Dr. H. Schönherr, Prof. Dr. G. J. Vancso

Department of Materials Science and Technology of Polymers  
MESA<sup>+</sup> Institute for Nanotechnology, University of Twente  
P.O. Box 217, 7500 AE Enschede (The Netherlands)  
Fax: (+31) 53-489-3823  
E-mail: g.j.vancso@utwente.nl

W. Shi, Prof. Dr. X. Zhang  
Key Lab of Organic Optoelectronics and Molecular Engineering  
Department of Chemistry, Tsinghua University  
Beijing 100084 (P.R. China)

[\*\*] The authors thank Dr. M. Péter and Dr. R. G. H. Lammertink for their contribution to the synthesis of PFS<sub>100</sub>, and Jing Song and Yujie Ma for their contributions and invaluable discussions. Financial support by the Netherlands Organization for Scientific Research (NWO Echo project 700.54.021; NWO middelgroot grant 700.54.102), the European Commission (IIF Marie Curie Fellowship, MIF1-CT-2004-008919), and the MESA<sup>+</sup> Institute for Nanotechnology is gratefully acknowledged.

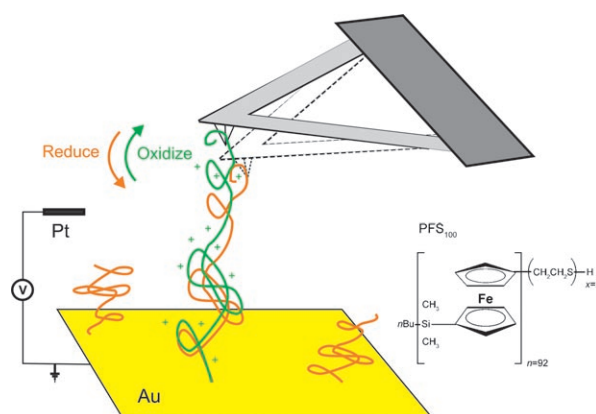


**Figure 1.** Stretching of single stimulus-responsive ethylene sulfide end-capped PFS (PFS<sub>100</sub>) chains by electrochemical AFM-based SMFS. The self-assembled monolayer (SAM) of 11-mercapto-1-undecanol (C11OH) has been omitted for clarity.

future development of optimized electrochemically driven single-chain polymer devices.

The experiments were based on the previously established self-assembled monolayer (SAM) platform obtained by insertion and subsequent stable attachment of ethylene sulfide end-capped PFS (PFS<sub>100</sub>) in SAMs of 11-mercapto-1-undecanol (C11OH) on gold electrodes.<sup>[17]</sup> Coverage values of  $6.2 \times 10^{-4}$  molecules nm<sup>-2</sup> (that is, on average one PFS<sub>100</sub> molecule on ca. 1600 nm<sup>2</sup>) ensured that individual PFS macromolecules were probed in AFM force–displacement (f–d) experiments (Figure 1).

The SMFS measurements were carried out under controlled electrochemical potential in an electrochemical AFM liquid cell filled with NaClO<sub>4</sub> (0.1 mol L<sup>-1</sup>) electrolyte solution. The SMFS experiment was conducted such that the AFM tip was repeatedly approached very close to the substrate surface (<2 nm) and retracted to a distance of 80 nm from the substrate. If a PFS chain was indeed physisorbed on the tip, a restoring force was detected upon retraction.<sup>[18]</sup> The single-chain elasticity of such a bridging chain was subsequently probed, typically up to five times (before desorption), in consecutive deflection–displacement curves (which are readily converted into force–extension ( $D$ – $\epsilon$ ) curves; Figure 2a), in which the pulling force was limited to values below the mean contact rupture force of  $0.35 \pm 0.15$  nN.<sup>[19]</sup> The stretching of individual chains was ensured

by careful analyses of all f–d curves captured, including the verification of the superposition of different normalized force–extension curves.<sup>[20]</sup> The raw data shown in Figure 2a also provide evidence for the reversibility of the stretching and relaxation processes<sup>[21]</sup> and the absence of chain slip or debonding from the AFM tip.<sup>[22]</sup>

Individual PFS chains kept in an extended state between the AFM tip and electrode surface were electrochemically oxidized at constant  $z$  position by applying a potential of +0.5 V followed by deflection–displacement measurements under constant potential (Figure 2c, cycle 1). The complete oxidation of the PFS chains on the gold working electrode was evident from the cyclic voltammetry (CV) data captured in situ. The first peak arises from the initial oxidation of alternating ferrocene units, followed by oxidation of the ferrocene centers in between at a higher potential (second peak) as a result of charge polarization of the neighboring ferrocene centers in the polymer, both through the SiR<sub>2</sub> groups and through space (Figure 2c, inset).<sup>[23]</sup> Similarly, single chains were stretched in the oxidized state, followed by electrochemical reduction at constant  $z$  position and continued force spectroscopy (Figure 2d, cycle 2).

In the experiments it was observed that the force at fixed maximum extension decreased upon oxidation and increased upon reduction to the neutral state. Thus, the change in the redox states is directly coupled to a mechanical output signal

of the force sensor (for cycle 1:  $\approx 200$  pN). The offset of the two curves shown in Figure 2d is attributed to thermal drift (the deflection of 3.5 nm corresponds to a change in temperature of ca. 0.035 °C)<sup>[24]</sup> during the course of the experiment (the delay time between capturing the two curves was 13 s). Coincidentally, no offset was observed for the curves shown in Figure 2c.

Similar to our earlier study,<sup>[13,14]</sup> typical cycles, such as the one depicted in Figure 2 (raw data), were converted into force–extension curves (Figure 3a and b). The mean force value at extensions below 10 nm was chosen as reference (zero) in each force curve. The observation of a lengthening of the oxidized chain with respect to the neutral chain, which is in line with the data shown in Figure 2c and d, can be attributed to the electrostatic repulsion among the oxidized ferrocene centers along the chain.<sup>[25]</sup> The two data sets display the entire mechanoelectrochemical cycle for two individual mole-

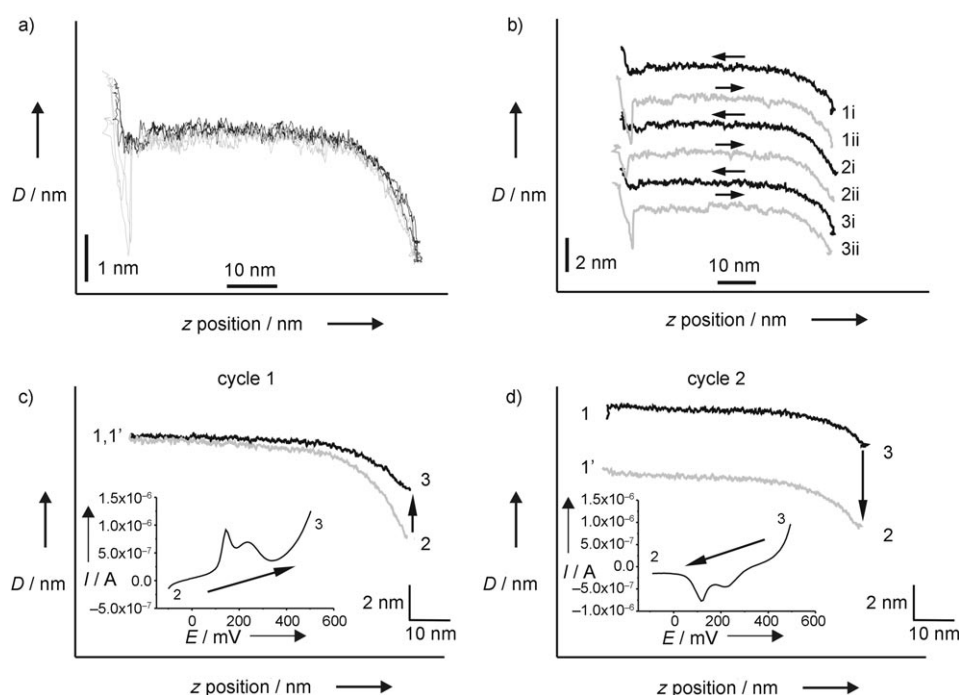


**Figure 2.** Raw SMFS deflection ( $D$ )–displacement data captured in NaClO<sub>4</sub> electrolyte solution. a) Three successive stretch–relax series measured on a single PFS<sub>100</sub> chain. b) The same data as in (a), where the curves have been offset vertically for clarity. c) A single neutral PFS<sub>100</sub> chain was stretched and oxidized under tension, followed by relaxation to the unstretched state (cycle 1; black line: oxidized PFS; gray line: neutral PFS; the sequence was 1–2–3–1'). d) A single oxidized PFS<sub>100</sub> chain was stretched and reduced under tension, followed by relaxation to the unstretched state (cycle 2; black line: oxidized PFS; gray line: neutral PFS; the sequence was 1–3–2–1'). The insets in (c) and (d) show the CV data captured during ramping of the applied potential.<sup>[23]</sup> All SMFS measurements were performed under a constant applied potential of  $-0.1$  or  $+0.5$  V for the reduced and oxidized forms, respectively.

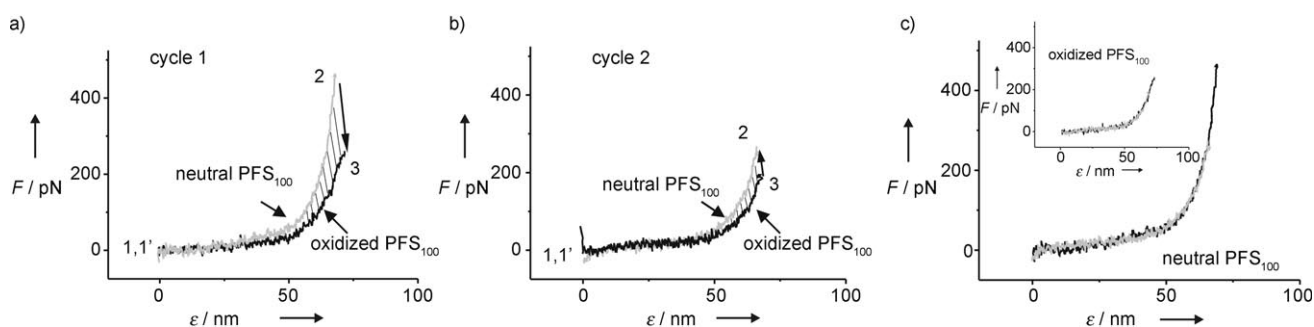


**Figure 3.** Force–extension ( $F$ – $\epsilon$ ) curves of a) cycle 1 and b) cycle 2. The enclosed areas of the cycles correspond to the mechanical work input or output of the single-polymer-chain mechanochemical cycle. c) The force–extension curves for the neutral and oxidized (inset) states for both cycles (black lines: data from cycle 1; gray lines: data from cycle 2) superimpose well, which indicates that single chains with the same contour length were stretched.

cules in both possible directions. As the two chains possess, within experimental error, the same length of 63 nm at a force value of 200 pN when they were neutral (Figure 3c), the data can be directly compared.

The areas enclosed between the corresponding curves for the oxidized and reduced  $\text{PFS}_{100}$  macromolecules in cycles 1 and 2 correspond to the work input ( $W_{\text{in}}$ ) and work output ( $W_{\text{out}}$ ) of the electromechanical cycles, respectively. As the change of the electrochemical potential  $\Delta\mu$  [Eq. (1); where  $\bar{\mu}_i$  is the chemical potential of the electrochemically oxidized PFS chain,  $\mu_i$  is the chemical potential of the neutral PFS chain,  $z_i$  is the number of charges per redox center ( $z_i = 1$ ),  $F$  is the Faraday constant ( $96486 \text{ C mol}^{-1}$ ), and  $\Delta\phi$  is the electric potential required to complete the oxidation/reduction of the entire PFS chain] and the number of transferred charges  $\Delta N$  during the oxidation/reduction processes are known, the efficiency  $\eta$  of the single-molecule electromechanical cycle can be estimated [Eq. (2); where  $W = W_{\text{out}} = -W_{\text{in}}$ ].<sup>[13]</sup>

$$\text{cycle 1: } \Delta\mu = \bar{\mu}_i - \mu_i = z_i F \Delta\phi \quad (1)$$

$$\text{cycle 2: } \Delta\mu = \mu_i - \bar{\mu}_i = z_i F \Delta\phi$$

$$\eta = \frac{W}{|\Delta\mu| \Delta N} \quad (2)$$

Ignoring the data for forces below 30 pN, for cycle 1  $W$  was estimated to be  $2.2 \times 10^{-18} \text{ J}$  for an extension from 40 to 68 nm, while for cycle 2,  $W$  was  $0.7 \times 10^{-18} \text{ J}$  for an extension from 40 to 66 nm. The corresponding efficiencies of cycles 1 and 2 (Figure 3a and b) can be estimated as 26 and 8%, respectively. The difference in the numerical values originates from the different maximum extension of the chain as a consequence of the different maximum forces applied in the experiments. In addition, cycle 2 shows a deviation from the expected plateau at extensions below 50 nm, which is a consequence of minor laser-light interference effects and an increased noise level observed for the oxidized curve. As a result, the enclosed area for extensions below 40 nm is negligible and does not contribute to  $W$ . It is important to consider that the efficiency values obtained from cycles 1 and 2 are calculated by assuming idealized conditions of energy input, that is, no dissipative processes take place, which may lead to an overestimation of these values.

Assuming a constant potential, the relation between stretching ratio (defined as the ratio between extension  $\epsilon$  for the neutral chain and maximum extension realized experimentally for the neutral chain in cycle 1,  $\epsilon_{\text{max}}^1$ ) can be evaluated from Figure 3a. The corresponding plot shows a monotonically increasing relationship between efficiency and stretching ratio (Figure 4). The mean attainable efficiency

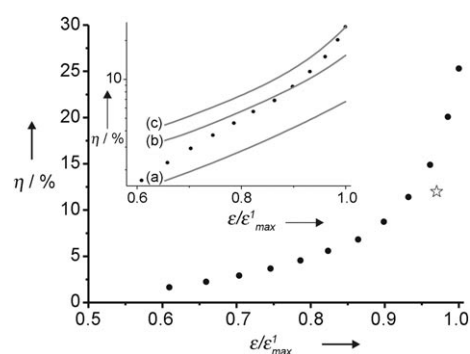


**Figure 4.** Efficiency of the closed-loop mechanochemical cycle of an individual  $\text{PFS}_{100}$  macromolecule versus stretching ratio ( $\epsilon/\epsilon_{\text{max}}^1$ ) calculated from the data of cycle 1 by integration of the area enclosed between the curves for different  $\epsilon$  values. The star shows the efficiency of a different macromolecule (data converted from cycle 2). Inset: logarithmic plot of the predictions of the efficiency versus stretching ratio for cycles of a macromolecule that changes from state 1 to different final states 2, where the Kuhn length  $l_k$  and segment elasticity  $K_s$  parameters from the m-FJC model for state 2 were varied by a) 20, b) 50, and c) 80% (see text for details).

under the experimental conditions used is estimated to be on the order of 20% (based on the determined mean rupture force of 0.35 nN<sup>[19]</sup>). The efficiency of cycle 2, corrected for the mentioned underestimate of  $\eta$  for extensions below 40 nm, was also plotted in the corresponding graph (by assuming identical contour lengths). A good agreement of the efficiencies measured for these individual molecules is obtained within experimental error. Hence, we observed the same efficiency for both directions of the closed electro-mechanical cycle.

The inset in Figure 4 shows a logarithmic plot calculated based on the modified freely jointed chain (m-FJC) model of

efficiency versus stretching ratio for cycles of a macromolecule that changes from state 1 to different final states 2, for which different elasticity parameters of the m-FJC model were assumed (20, 50 and 80 % increase in the Kuhn length  $l_K$  and a corresponding decrease in the segment elasticity  $K_s$ ). The maximum efficiency is critically influenced by the variation in elasticity that can be achieved through the external stimulus, that is, 7, 15 and 26 % for a systematic change in  $l_K$  (increase) and  $K_s$  (decrease) of 20, 50 and 80 %, respectively. The experimental results from cycle 1 for PFS<sub>100</sub> are also included in the graph.

Compared with our previous report,<sup>[13,14]</sup> in which the force–extension curves were described in both oxidation states by the m-FJC model<sup>[26]</sup> and in which the efficiency was then calculated for a loop with isoforce transitions, we now observe an increased efficiency. The difference can be attributed to the facts that 1) the force values previously considered ranged from 20 to only 140 pN, 2) the change in the oxidation state was assumed to occur under the condition of constant force, and 3) the numerical values of the current fit parameters of the m-FJC model (for oxidized PFS<sub>100</sub>,  $l_K = 0.41$  nm,  $K_s = 4.9$  nN nm<sup>−1</sup>; for neutral PFS<sub>100</sub>,  $l_K = 0.26$  nm;  $K_s = 28.4$  nN nm<sup>−1</sup>) differ slightly from the previous ones, as we evaluated curves with higher force and extension values.<sup>[27]</sup> If we evaluate the current data in a similar manner as previously, a mechanical work of  $0.8 \times 10^{-18}$  J and an efficiency of 9.4 % are found. In addition, we emphasize that the results given here are not statistically averaged data but single-molecule data, that is, we sampled individual molecules.

In conclusion, closed mechanochemical cycles of single PFS<sub>100</sub> chains were obtained by using electrochemical SMFS. A chain lengthening of oxidized with respect to neutral chains was observed, which is attributed to the electrostatic repulsion between the oxidized ferrocene centers along the chain. A force of ca. 200 pN on the AFM cantilever was detected upon redox stimulation, while a single prestretched PFS<sub>100</sub> chain was held at a constant  $z$  position. Electro-mechanical cycles were completed in both directions as closed loops and showed comparable efficiencies. The single-chain efficiency was found to increase with increasing stretching ratio. Experimentally, a maximum efficiency of 26 % was observed.

## Experimental Section

**Materials:** C11OH and PFS<sub>100</sub>, synthesized by anionic polymerization (number-average molecular weight  $M_n = 22\,600$  g mol<sup>−1</sup>, number-average degree of polymerization  $DP_n = 92$ , weight-average molecular weight  $M_w/M_n = 1.13$ ), were available from previous studies.<sup>[13,14]</sup> Gold substrates (Ssens B.V., Hengelo, The Netherlands) were cleaned in piranha solution (H<sub>2</sub>SO<sub>4</sub>/30 % H<sub>2</sub>O<sub>2</sub> (7:3, by volume) [Caution: piranha solution should be handled with extreme care; it has been reported to detonate unexpectedly], then rinsed with copious amounts of Milli-Q water and ethanol, followed by drying in a nitrogen stream. These substrates were immersed overnight in a solution of C11OH in ethanol ( $2.5 \times 10^{-3}$  mol L<sup>−1</sup>), followed by rinsing with ethanol and immersion in a solution of PFS<sub>100</sub> in toluene ( $0.2 \times 10^{-3}$  mol L<sup>−1</sup>) for 2 min.<sup>[16]</sup> Subsequently, the samples were cleaned by placing them in neat toluene and dichloromethane for 10 min each, followed by drying in a stream of nitrogen.<sup>[17]</sup>

Force spectroscopy experiments were performed with a Pico-Force AFM instrument running on a NanoScope IVa controller (Veeco/Digital Instruments (DI), Santa Barbara, CA) equipped with an electrochemical liquid cell (volume ca. 50  $\mu$ L; DI) and commercially available V-shaped Si<sub>3</sub>N<sub>4</sub> cantilevers (DI). Each cantilever was calibrated before a given experiment by measuring and analyzing the thermal excitation spectrum.<sup>[28]</sup> The measured spring constants of the cantilevers varied between 0.06 and 0.10 ( $\pm 0.017$ ) N m<sup>−1</sup>. For the electrochemical SMFS experiments, the electrochemical liquid cell was interfaced with an external Autolab PGSTAT10 potentiostat (EcoChemie, Utrecht, The Netherlands). The PFS<sub>100</sub>-covered gold substrate was the working electrode; Pt wires were used both as reference and counter electrodes.<sup>[13]</sup> Cyclic voltammograms were recorded in aqueous solutions of NaClO<sub>4</sub> (0.1 mol L<sup>−1</sup>) between  $-0.1$  and  $+0.5$  V<sub>pt</sub> at a scan rate of 50 or 150 mV s<sup>−1</sup>. An external potential of  $+0.5$  V was held during the force measurements to ensure the complete oxidation of PFS molecules. For reduction the potential was set to  $-0.1$  V.

Received: June 1, 2007

Published online: October 1, 2007

**Keywords:** atomic force microscopy · electrochemistry · molecular motors · polymers · single-molecule studies

- [1] a) H. Y. Wang, G. Oster, *Nature* **1998**, *396*, 279–282; b) P. D. Boyer, *Annu. Rev. Biochem.* **1997**, *66*, 717–749.
- [2] L. Mahadevan, P. Matsudaira, *Science* **2000**, *288*, 95–99.
- [3] T. Atsumi, L. McCarter, Y. Imae, *Nature* **1992**, *355*, 182–184.
- [4] a) D. D. Hackney, *Science* **2007**, *316*, 58–59; b) M. C. Alonso, D. R. Drummond, S. Kain, J. Hoeng, L. Amos, R. A. Cross, *Science* **2007**, *316*, 120–123.
- [5] H. Hess, G. D. Bachand, V. Vogel, *Chem. Eur. J.* **2004**, *10*, 2110–2116.
- [6] a) A. P. Davis, *Nature* **1999**, *401*, 120–121; b) S. Saha, J. F. Stoddart, *Chem. Soc. Rev.* **2007**, *36*, 77–92.
- [7] A. R. Pease, J. O. Jeppesen, J. F. Stoddart, Y. Luo, C. P. Collier, J. R. Heath, *Acc. Chem. Res.* **2001**, *34*, 433–444.
- [8] W. R. Browne, B. L. Feringa, *Nat. Nanotechnol.* **2006**, *1*, 25–35.
- [9] S. P. Fletcher, F. Dumur, M. M. Pollard, B. L. Feringa, *Science* **2005**, *310*, 80–82.
- [10] T. Hugel, N. B. Holland, A. Cattani, L. Moroder, M. Seitz, H. E. Gaub, *Science* **2002**, *296*, 1103–1106.
- [11] a) D. A. Foucher, R. Ziembinski, B. Z. Tang, P. M. Macdonald, J. Massey, C. R. Jaeger, G. J. Vancso, I. Manners, *Macromolecules* **1993**, *26*, 2878–2884; b) *Metal-Containing and Metallosupramolecular Polymers and Materials* (Eds.: U. S. Schubert, G. R. Newkome, I. Manners), American Chemical Society, Washington, **2006**.
- [12] a) M. Péter, M. A. Hempenius, E. S. Kooij, T. A. Jenkins, S. J. Roser, W. Knoll, G. J. Vancso, *Langmuir* **2004**, *20*, 891–897; b) M. Péter, R. G. H. Lammertink, M. A. Hempenius, G. J. Vancso, *Langmuir* **2005**, *21*, 5115–5123.
- [13] S. Zou, M. A. Hempenius, H. Schönherr, G. J. Vancso, *Macromol. Rapid Commun.* **2006**, *27*, 103–108.
- [14] S. Zou, I. Korczagin, M. A. Hempenius, H. Schönherr, G. J. Vancso, *Polymer* **2006**, *47*, 2483–2492.
- [15] W. Q. Shi, S. Cui, C. Wang, L. Wang, X. Zhang, X. J. Wang, L. Wang, *Macromolecules* **2004**, *37*, 1839–1842.
- [16] H. J. Butt, *Macromol. Chem. Phys.* **2006**, *207*, 573–575.
- [17] S. Zou, Y. Ma, M. A. Hempenius, H. Schönherr, G. J. Vancso, *Langmuir* **2004**, *20*, 6278–6287.
- [18] Polymer chains were also successfully stretched if the tip touched the surface; see, for example, Figure 2a.
- [19] Contact rupture force refers to breaking of the weakest link (polymer–AFM tip desorption in this case).



- [20] W. Zhang, X. Zhang, *Prog. Polym. Sci.* **2003**, 28, 1271–1295.
  - [21] H. B. Li, W. K. Zhang, W. Q. Xu, X. Zhang, *Macromolecules* **2000**, 33, 465–469.
  - [22] L. Sonnenberg, J. Parvole, O. Borisov, L. Billon, H. E. Gaub, M. Seitz, *Macromolecules* **2006**, 39, 281–288.
  - [23] D. A. Foucher, B. Z. Tang, I. Manners, *J. Am. Chem. Soc.* **1992**, 114, 6246–6248.
  - [24] Unpublished results.
  - [25] a) T. Odijk, *Macromolecules* **1979**, 12, 688–693; b) J. Skolnick, M. Fixman, *Macromolecules* **1977**, 10, 944–948.
  - [26] The Kuhn length and segment elasticities according to the m-FJC model used in reference [13] for neutral and oxidized PFS<sub>100</sub> were 0.38 and 0.65 nm, and 30 and 45 nN nm<sup>−1</sup>, respectively.
  - [27] The dependence of the fit parameters on the magnitude of the extension and force is well known; see, for example: T. Hugel, M. Grosholz, H. Clausen-Schaumann, A. Pfau, H. E. Gaub, M. Seitz, *Macromolecules* **2001**, 34, 1039–1047.
  - [28] H. J. Butt, M. Jaschke, *Nanotechnology* **1995**, 6, 1–7.
-